JOC The Journal of Organic Chemistry
Cite This: J. Org. Chem. 2019, 84, 11268−11274
Note
pubs.acs.org/joc

Complementary Synthetic Approaches toward 9-Phosphatriptycene and Structure−Reactivity Investigations of Its Association with Sterically Hindered Lewis Acids

Lei Hu,[§,‡] Damien Mahaut,[§] Nikolay Tumanov,[§] Johan Wouters,[§] Raphaël Robiette,*[,‡] and Guillaume Berionni*[,§]

[§]Department of Chemistry, Namur Institute of Structured Matter, University of Namur, rue de Bruxelles 61, 5000 Namur, Belgium
[‡]Institute of Condensed Matter and Nanosciences, Université catholique de Louvain, Place Louis Pasteur 1 Box L4.01.02, 1348 Louvain-la-Neuve, Belgium

Supporting Information

ABSTRACT: Two practical and high-yielding syntheses of 9-phosphatriptycene are reported. In both approaches, the key step is based on the cyclization of a (tris)lithio-triphenylmethane or a (tris)lithio-triphenylphosphine intermediate on a phosphorus or a carbon electrophile, respectively. The association of 9-phosphatriptycene with representative boron- and carbon-centered Lewis acids was investigated by IR, NMR, and UV−vis titration experiments and by computational methods, shedding light on its steric hindrance, σ-donating ability, and Brønsted and Lewis basicities.

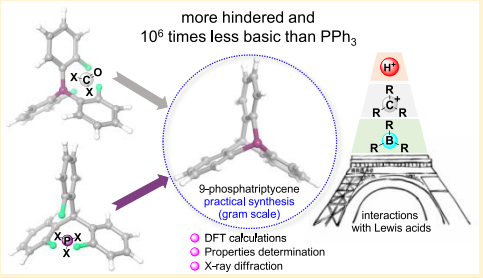

Phosphines are ubiquitous Lewis bases and prototypical ligands for transition metals with numerous applications in transition-metal catalysis,[1] organocatalysis,[2] and frustrated Lewis pair chemistry.[3]

While the stereoelectronic properties of phosphines are generally tuned by varying the substitution pattern of their alkyl or aryl substituents,[4] modulation of their properties by varying the trivalent phosphorus atom pyramidalization via a structural constraint has been much less studied.[5] Among these geometrically constrained phosphines (Figure 1a), the cage-shaped 9-phosphatriptycenes **1**−**2**[6] and the 10-hetero-9-phospha-triptycenes **3**−**6** (Figure 1b) are of growing interest in catalysis.

Phosphatriptycenes are known to possess a phosphorus lone pair with a high s-character and a low σ-donor character.[6b,7b] Phosphatriptycene derivatives **3**−**6** have been recently employed as efficient ligands in palladium-catalyzed cross-coupling reactions,[7,8] in hydroformylations of alkenes,[9] and as ligands for the design of new transition-metal complexes.[10,11]

Their Brønsted and Lewis basicities have been however nearly unexplored, and the association of the parent 9-phosphatriptycene (**1**) with Lewis acids has not been investigated so far.

Herein, we report a combined computational and experimental study of its σ-donating ability and reactivity with a series of Lewis acids of small (H^+, CH_3^+, BF_3) and large ($B(C_6F_5)_3$, CPh_3^+) sizes for shedding light on its stereoelectronic properties. We have also developed new practical pathways to overcome the limitations and low-yielding steps of the original 6 steps synthesis of **1**,[6a] which is currently limiting its widespread uses in catalysis (Scheme 1).

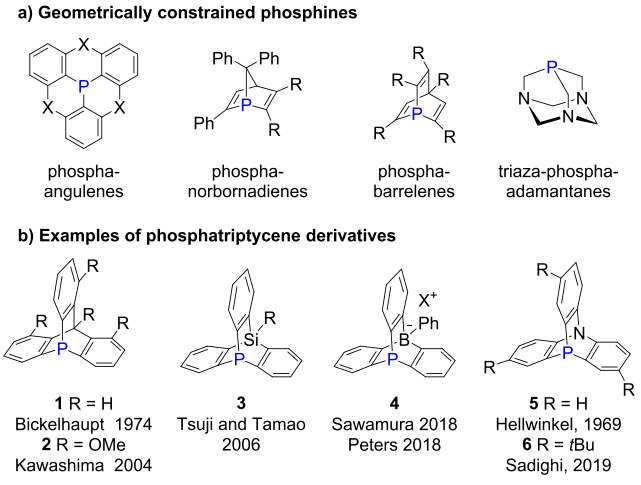

Figure 1. Representative classes of geometrically constrained phosphines and of cage-shaped phosphatriptycene derivatives.

Inspired by previous approaches from Bickelhaupt,[6a] Kawashima,[6c] and Sadighi,[12] we obtained **1** from the tris(*ortho*-bromo)-triphenylphosphine **7** in three steps (Scheme 2).

In contrast with the unsuccessful attempts of Hellwinkel to obtain **1** from (tris)halogeno-trityl precursors,[13] we also succeeded in synthesizing **1** in a good yield by a triple

Received: June 13, 2019
Published: August 6, 2019

DOI: 10.1021/acs.joc.9b01570
J. Org. Chem. 2019, 84, 11268−11274

Scheme 1. (a) Original 9-Phosphatriptycene Synthesis[6a] and (b) New Synthetic Approaches Proposed in This Work

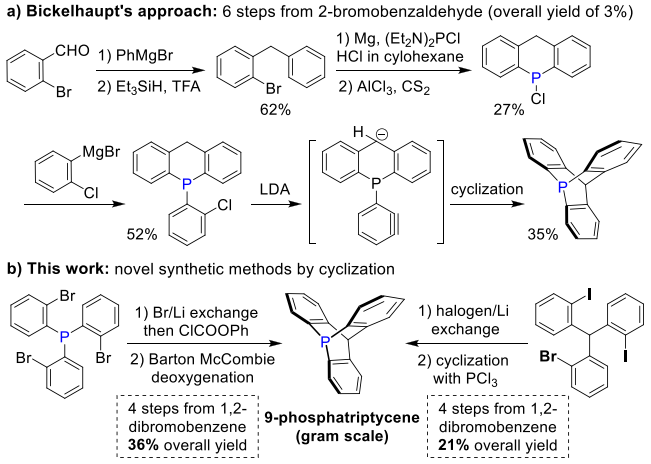

Scheme 2. Synthesis of 9-Phosphatriptycene 1 Starting from 7

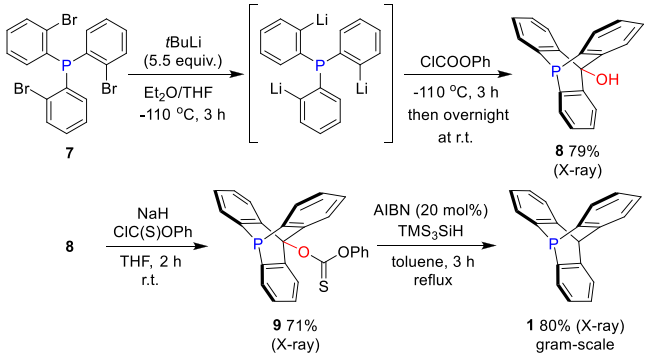

Scheme 3. Synthesis of 9-Phosphatriptycene 1 Starting from the Halogenated Triphenylmethane Precursor 10

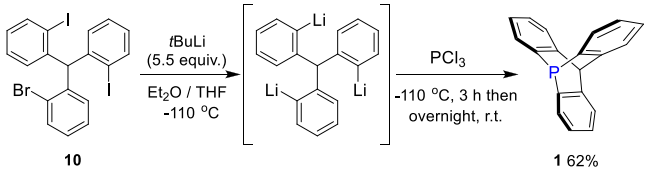

halogen/lithium exchange on **10**[14] followed by treatment with PCl_3 (Scheme 3).

Though very few structures with O−H···P hydrogen bonds are reported, we observed by single-crystal X-ray diffraction a short O−H···P hydrogen bond (H···P length of 2.71(3) Å) in the solid-state structure of the synthetic intermediate **8** (Figure 2). The triptycene scaffolds formed a linear arrangement with an eclipsed supramolecular conformation and with a π-stacking distance of 3.796 Å between their adjacent parallel aryl rings.

Based on the X-ray structure of 9-phosphatriptycene **1** measured at various temperatures with higher structural accuracy than in the previously reported structure,[6a] its crystallographic cone angle[15] was determined to be 162°, comparable to that of Cy_3P(160°), to **3** (165°)[7] and **4** (157°),[8a] suggesting that **1** is more hindered than PPh_3 (Table 1).

Since cone angle measurements provide a spherical measure of sterics, whereas **1** showed a nonspherical distribution of

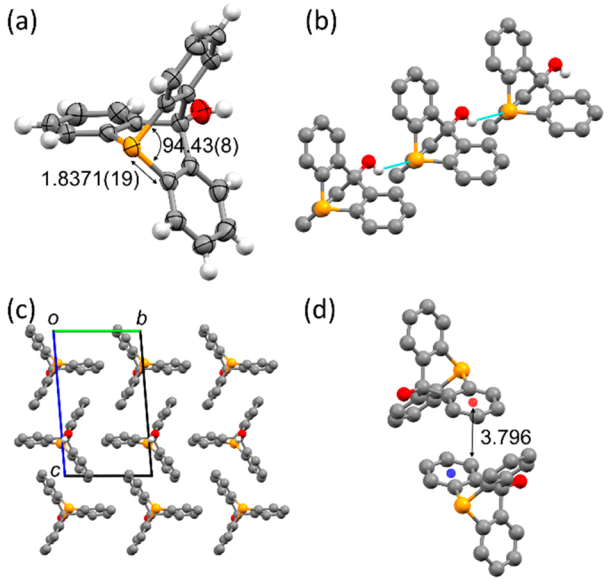

Figure 2. (a) Molecular geometry of **8** and its crystal packing: (b) chains, (c) cell view, and (d) $\pi-\pi$ stacking. H atoms are omitted for clarity.

Table 1. Computed[19] and Experimental Stereoelectronic Descriptors for 9-Phosphatriptycene (1) and for PPh_3 (11)

parameters	P-trip 1	PPh_3 11
cone angle (deg)	160[a]	148[a,b]
average C−P−C angle (deg)	94.7[a]	102.2[a]
He_8_steric (kcal/mol)	9.3	8.0
$E_{lone\ pair}$ (Hartree)	−0.4336	−0.3889
charge on P	0.8586	0.8787
LP s-character (%)[c]	56.1	50.9
ν_{CO}/Rh (cm^{-1})[a]	1985[a]	1976[a]
PA (kcal/mol)[d]	251.6	264.2
MCA (kcal/mol)[d]	111.8	122.4

[a]Experimental values. [b]See ref 15b. [c]LP s-character is the contribution of P s-orbital to the lone pair. [d]PA and MCA stand for proton affinity and methyl cation affinity.

steric bulk, we computed its He_8_steric parameter,[16] a well-established parameter describing the steric interaction energy of phosphine ligands with a planar surface (see the Supporting Information). The obtained He_8_steric of 9.3 kcal/mol for **1** confirmed that it is bulkier than PPh_3 (He_8_steric = 8.0 kcal/mol).

Next, we investigated the electronic properties of **1**. NBO analysis revealed a lower energy of the lone pair on phosphorus ($E_{lone\ pair}$) in **1** than in PPh_3 (Table 1), with a higher contribution of P s-orbital to the lone pair than in PPh_3.[17] The experimental IR stretching frequency (ν_{CO}) in the Rh(acac)-CO(9-phosphatriptycene) complex is equal to 1985 cm^{-1}, almost identical as in the *para*-CF_3-triphenylphosphine complex (1986 cm^{-1}).[18] These results indicate that **1** is a very weak electron-donating ligand.

In line with these data, the proton affinity (PA) of **1** was computed to be ca. 10 kcal/mol lower than for PPh_3 (Table 1). Linear correlation of PA versus pK_a (H_2O) of representative triarylphosphines provided a pK_a (H_2O) of −1.5(5) for **1** (see the Supporting Information), about 5 orders of magnitude less basic than PPh_3 (pK_a (H_2O) = 3.28)[20] and comparable to the *para*-CF_3-triphenylphosphine (pK_a (H_2O) = −1.39).[20]

DOI: 10.1021/acs.joc.9b01570
J. Org. Chem. 2019, 84, 11268−11274

The Lewis basicity of **1** with respect to carbon-centered Lewis acids[21] was determined by measuring the equilibrium constant of association of **1** with benzhydrylium ions **12a–b** of calibrated Lewis acidity parameters (Scheme 4).

Scheme 4. Association of 1 with Benzhydrylium Ions 12a–b and Corresponding ^{31}P Chemical Shifts in CD_3CN

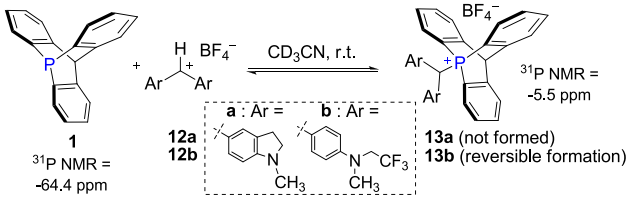

Whereas the association of **1** with the weak benzhydrylium Lewis acid **12a** (LA = −6.33) was not observed (Lewis adduct **13a** not detected by ^{1}H or ^{31}P NMR), its association with the 10^6 times more Lewis acidic benzhydrylium ion **12b** (LA = −0.83)[21a] was found to be highly reversible.

From the ratio of the respective ^{1}H NMR signals of **1**, **12b**, and the resulting adduct **13b** at the equilibrium, an association constant of K = 20.03 was measured in CD_3CN. This value provided a Lewis basicity parameter of LB = 7.63 for **1**, indicating that it is a 10^6 times weaker Lewis base than PPh_3 (LB = 14.27 in CH_3CN, Figure 3).[21] This is also supported by the lower methyl cation affinity for **1** as compared to PPh_3 (Table 1).

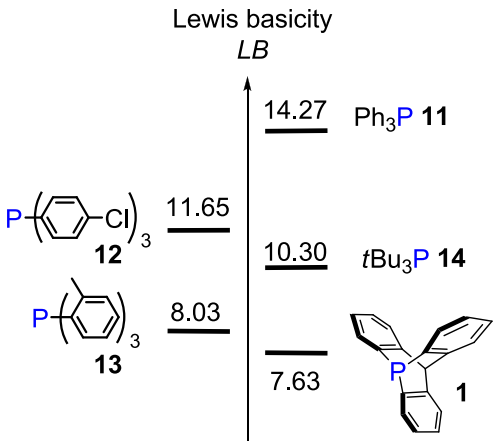

Figure 3. Lewis basicity scale toward benzhydrylium ions for selected phosphines. Lewis basicity parameters LB values for **11–14** in CH_3CN from ref 21c.

Though **1** has a larger cone angle and is 10^6 times less basic than PPh_3, it quantitatively associated with the sterically hindered tritylium ion **15** and with tris(pentafluorophenyl)-borane **17** (Scheme 5) showing that steric repulsions do not prevent an exergonic Lewis adduct formation process.

Counterintuitively, structural analysis of the Lewis adducts **16** and **18** showed that even if the P atom of **1** is included in a tricyclic cage-shaped scaffold, which infer a high structural rigidity, the C–P–C angle in phosphatriptycene moiety decreased by 4° upon Lewis acid coordination, even more than in the case of PPh_3 (3.0°). The CPh_3 and $B(C_6F_5)_3$ moieties in the adducts **16** and **18** adopted a gauche eclipsed

Scheme 5. Association of 1 with the Sterically Hindered Lewis Acids CPh_3^+ 15 and $B(C_6F_5)_3$ 17[a]

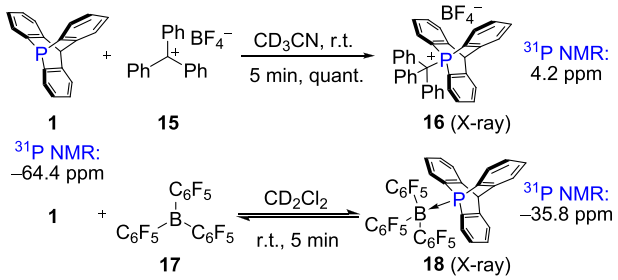

[a]For the X-ray structures of **16** and **18**, see the Supporting Information.

conformation with a small dihedral angle rather than a staggered conformation (Figure 4).

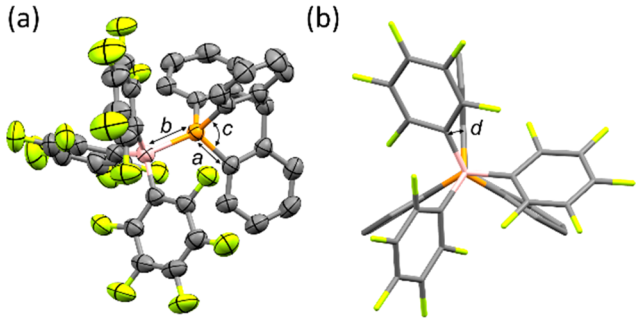

Figure 4. Molecular geometry of the Lewis adduct **18** represented under two orientations. H atoms and solvent are omitted. (a) Ellipsoid representation at the 50% probability level. (b) Top view. Selected geometrical parameters: a = 1.833(2) Å, b = 2.125(2) Å, c = 98.7°, d = 24.9°.

In order to rationalize these unexpected structural features, we investigated the association of **1** with a series of boron Lewis acids varying by their Lewis acidity and steric bulk (BF_3, BPh_3, and $B(C_6F_5)_3$) by computing its complexation free energy and analyzing the Lewis adduct structures (Table 2).

Table 2. Computed[19] Free Energy of Complexation of 1 and PPh_3 with Boron Lewis Acids[a]

Lewis adducts	ΔG^0_{calcd} (kcal/mol)	P–B bond distance (Å)	ΔC–P–C (deg)[b]
1-BF_3 (**19**)	5.0	2.091	4.2
1-BPh_3 (**20**)	1.4	2.104	3.0
1-$B(C_6F_5)_3$(**18**)	−7.6 [−6.3]	2.127 [2.125(2)]	3.6 [4.0]
Ph_3P-BF_3(**22**)	−0.5	2.083	5.2
Ph_3P-BPh_3(**23**)	−0.4	2.154	3.0
Ph_3P–$B(C_6F_5)_3$ (**24**)	−7.1	2.257 [2.180(6)]	3.0 [2.8]

[a]Experimental values obtained by X-ray diffraction analysis in brackets. [b]Change in C–P–C angle compared to free phosphine.

The computed ΔG°_{calcd} value for **1** with $B(C_6F_5)_3$ (−7.6 kcal/mol) was in good agreement with the measured association constant of 4.7 × 10^4 L mol^{-1}, corresponding to a ΔG°_{exp} of −6.3 kcal/mol.

Computed complexation free energies (ΔG°_{calcd}) of **1** with BF_3 are found to be endergonic (+5.0 kcal/mol) in line with

DOI: 10.1021/acs.joc.9b01570
J. Org. Chem. 2019, 84, 11268–11274

the lower Lewis basicity of **1** compared to PPh_3. However, increasing the size of the borane Lewis acid leads to an unexpected attenuation of complexation free energies difference between **1** and PPh_3. Indeed, for $B(C_6F_5)_3$, complexation with **1** and PPh_3 is similarly favored (see Table 2).

A detailed structural and electronic analysis of Lewis adducts **16** and **18** revealed that this observation can be accounted for the C3 symmetry of 9-phosphatriptycene, which presents three C−H, pointing toward the $B(C_6F_5)_3$ Lewis acid subunit, allowing C−H···F and C−H···π stabilizing interactions in the complex **18** (see Supporting Information for full details). In the case of PPh_3, the three aromatic rings on the phosphine adopt a helicoidal conformation (to decrease the steric clashes between these three aromatic rings) leading to lower noncovalent stabilizing interactions between the two partners. This increased stabilization by noncovalent interactions in the case of **1** is also reflected by the shorter P−B bond length in the adduct **18** (2.125(2) Å) than in the PPh_3 complex **24** (2.180(6) Å).

In summary, two practical and high-yielding synthetic approaches to access 9-phosphatriptycene in gram-scale quantities have been developed. Experimental and computational studies of the steric and electronic properties of 9-phosphatriptycene showed that this phosphine is more sterically hindered and a 10^6 times weaker Lewis and Brønsted base than PPh_3. Due to stabilizing noncovalent interactions, the association of $B(C_6F_5)_3$ with 9-phosphatriptycene is however as exergonic as with PPh_3 (Table 2) and was determined to be partially reversible at high dilutions. This Lewis acid/base pair may open new avenues in the field of frustrated Lewis pairs catalysis.

EXPERIMENTAL SECTION

General Information. All reactions were carried out using purified and dried solvents in a Schlenk flask under an argon or nitrogen atmosphere. Dichloromethane (DCM), diethyl ether (Et_2O), tetrahydrofuran (THF), and toluene were dried over a Pure Solv solvent purification system. Thin-layer chromatography was performed using Merck aluminum silica gel TLC plates and monitored by UV light at 254 nm. Flash chromatography separations were carried out using Merck silica gel (60, particle size 40−63 μm) with silica gel columns. Melting points were measured on a Büchi Melting Point B-545 instrument. ^1H and ^{13}C nuclear magnetic resonance (NMR) spectra were obtained on a JEOL ECX 400 or 500 MHz instrument in $CDCl_3$ or $CDCl_2$ or CD_3CN. Chemical shifts (δ) are reported in ppm and referenced indirectly to residual solvent signals. COSY, HSQC, and HMBC 2D NMR methods have been used to establish atom connectivity and attribution of signals. The IR spectra were acquired on a PerkinElmer Spectrum II FT-IR System UATR mounted with a diamond crystal on neat compounds between wavenumbers of 4000−450 cm^{-1}. High-resolution mass spectra (HRMS) were recorded on a Thermo Orbitrap Exactive device and performed by the molecular structural analysis (ASM) technological platform of UCLouvain. Previously reported compounds were synthesized according to literature procedures as described in the Supporting Information. Commercial reagents were used as received (>97% purity) from Sigma-Aldrich, ABCR, and FluoroChem. Tris(2-bromophenyl)-phosphine **7**[8a] and the trityl derivative **10**[14] were synthesized according to the methods reported in the literature.

Computational Studies. The bulk of the computations has been carried out using the Jaguar 8.5 pseudospectral program package.[22] All species have been fully geometry optimized, and the Cartesian coordinates are supplied in section 4.4 of the Supporting Information. The density functional theory (DFT) was applied by means of the B3LYP hybrid functional[23] corrected for dispersion as proposed by Grimme (D3 correction).[24] The standard split valence polarized 6-31+G(d) basis set[25] was used for all atoms. All optimization calculations were carried out using the polarizable continuum-Poisson method as incorporated in Jaguar, using the parameters for benzene, i.e., a dielectric constant of 2.284, and a solvent probe radius of 2.60 Å. Gas phase electronic energies were obtained after corresponding fully analytical single point calculations, at the M06-2X/6-311+G(d,p) level of theory. Solvation energies were obtained by single point calculations using the Poisson−Boltzmann polarizable continuum method as implemented in Jaguar, at the B3LYP-D3/6-31+G(d) level, using the parameters appropriate for benzene.

Thermal and entropic contributions to free energy were computed by performing frequency calculations at the B3LYP/6-31+G(d)-(benzene) level of theory. In Jaguar, the translational partition function is computed for ideal gas standard conditions, corresponding to a pressure of 1 atm at 298.15 K. For solution reactions, the standard condition is instead 1 mol/L. Accordingly, the free energy value computed in Jaguar was corrected by a concentration term, equal to RT ln (V_mol_gas_1 atm/V_mol_1M), i.e., 1.89 kcal/mol at 298.15 K.

We have made a systematic attempt to locate all possible local minima (at the B3LYP-D3/6-31+G(d) level), with the data presented referring to the lowest energy form. It can be noted that, in all cases, only a limited number of higher lying conformers was obtained (if any).

As described by Fey,[26] the He_8_steric parameters were computed by optimizing the phosphatriptycene (or PPh_3) geometry with its bridge-head phosphorus atom constrained to lie at 2.28 Å above the centroid, and perpendicular to the plane, of a helium ring, which is constituted by eight helium atoms with a 2.5 Å radius (see the Supporting Information).

Single-Crystal X-ray Diffraction Analysis. Single-crystal X-ray diffraction data for all compounds were collected on an Oxford Diffraction Gemini Ultra R diffractometer (4-circle kappa platform, Ruby CCD detector) using Mo Kα and Cu Kα radiation. Data collection, unit cells determination, and data reduction were carried out using the CrysAlis PRO software package.[27] All structure were solved with the SHELXT[28] structure solution program by Intrinsic Phasing methods and refined by full-matrix least-squares on $|F|^2$ using SHELXL-2018/3[29] with Olex2[30] and shelXle[31] as a shell. Non-hydrogen atoms were refined anisotropically. Hydrogen atoms were placed on calculated positions in riding mode with temperature factors fixed at 1.2 times U_{eq} of the parent carbon atoms (1.5 for methyl groups). The program Mercury[32] was used for molecular graphics.

Experimental Procedures and Product Characterization. *9-Phospha-10-hydroxytriptycene (**8**).* A 1.9 M solution of *t*BuLi (34 mL, 64.54 mmol, 4.0 equiv) in hexane was added dropwise to a solution of **7**[8a] (8.00 g, 16.13 mmol, 1.00 equiv) in THF/Et_2O (100 mL/100 mL) at −110 °C over 30 min, and the reaction mixture was stirred for 3 h at this temperature. A solution of phenyl chloroformate (2.0 mL in 10 mL of THF, 16.13 mmol, 1.00 equiv) was added dropwise to the reaction mixture over 30 min at −110 °C, and the reaction mixture was stirred for 3 additional hours at this temperature and was allowed to warm up to room temperature overnight. The reaction mixture was quenched with a saturated solution of NH_4Cl (2 mL), and the solvent was removed under reduced pressure. The resulting crude product was purified by flash chromatography on silica gel (cyclohexane/AcOEt = 15:1 to 5:1) to provide a colorless solid (3.67 g, 12.70 mmol, 79%). Crystals suitable for X-ray diffraction analysis were obtained by slow evaporation of a saturated solution of 9-phospha-10-hydroxytriptycene **8** in AcOEt. ^1H NMR (400 MHz, CD_2Cl_2): δ 7.81−7.72 (m, 6H, H-1, 8, 14, 4, 5, 11), 7.28 (ddd, J = 7.5, 4.9, 1.0 Hz, 3H, H-3, 6, 12), 7.16−7.08 (m, 3H, H-2, 7, 13). $^{13}C\{^1H\}$ NMR (100 MHz, CD_2Cl_2): δ 150.5 (d, J = 3.1 Hz, C-4a, 5a, 10a), 140.2 (d, J = 8.3 Hz, C-8a, 9a, 14a), 132.8 (d, J = 36.6 Hz, C-1, 8, 14), 128.9 (d, J = 1.5 Hz, C-3, 6, 12), 126.1 (d, J = 12.5 Hz, C-4, 5, 11), 121.5 (d, J = 0.8 Hz, C-2, 7, 13), 82.3 (d, J = 1.7 Hz, C-10). ^{31}P NMR (161 MHz, CD_2Cl_2): δ −72.27. HRMS (ESI$^+$): calcd for $C_{19}H_{14}OP$ $[M + H]^+$, 289.0777; found, 289.0777. Mp: 256−258 °C. TLC: R_f = 0.45 (hexane/AcOEt = 6:1, UV). IR: ν (neat, cm^{-1}) 3470,

DOI: 10.1021/acs.joc.9b01570
J. Org. Chem. 2019, 84, 11268−11274

3061, 2922, 2852, 1440, 1319, 1278, 1256, 1210 1164, 1132, 1110, 1094, 1056, 1049, 1026, 946, 904, 859, 758, 742, 700, 676, 633, 596, 542.

*9-Phospatriptycene-10-phenyl thiocarbonate (**9**).* To a stirred solution of 9-phospha-10-hydroxytriptycene **8** (3.67 g, 12.7 mmol, 1.00 equiv) in THF (150 mL) at room temperature was added NaH (60% dispersion in mineral oil, 0.61 g, 15.2 mmol, 1.20 equiv) portionwise. After 1 h at room temperature, phenylchlorothiocarbonate (2.10 mL, 15.2 mmol, 1.20 equiv) was added dropwise and the reaction mixture was stirred for 1 h. A saturated solution of NH_4Cl (50 mL) was added to quench the reaction, and the aqueous layer was extracted with CH_2Cl_2 (3 × 100 mL). The organic phase was washed with brine, dried over $MgSO_4$, filtered, and concentrated under reduced pressure. Purification of the crude product by flash chromatography using *n*-hexane/EtOAc (50:1) as an eluent afforded 9-phospatriptycene-10-phenyl thiocarbonate **9** (3.80 g, 8.96 mmol, 71%) as a pale yellow solid. Crystals suitable for X-ray diffraction analysis were obtained by slow evaporation of a saturated solution of 9-phospatriptycene-10-phenyl thiocarbonate **9** in AcOEt. ^{1}H NMR (400 MHz, $CDCl_3$): δ 8.06−7.72 (m, 6H, H-1, 4, 5, 8, 11, 14), 7.38 (app. t, J = 7.9 Hz, 2H, H-18, 20), 7.35−7.28 (m, 3H, H-3, 6, 12), 7.28−7.23 (m, 1H, H-19), 7.18−7.12 (m, 2H, H-17, 21), 7.12−7.05 (m, 3H, H-2, 7, 13). ^{13}C{^{1}H} NMR (100 MHz, CD_2Cl_2): δ 191.4 (C-15), 153.9 (C-16), 146.7 (d, J = 3.5 Hz, C-4a, 5a, 10a), 139.3 (d, J = 8.6 Hz, C-8a, 9a, 14a), 132.9 (d, J = 37.0 Hz, C-1, 8, 14), 130.3 (C-18, 20), 128.6 (d, J = 1.4 Hz, C-3, 6, 12), 127.6 (C-19), 126.5 (d, J = 12.5 Hz,, C-4, 5, 11), 123.7, 122.0 (C-17, 21), 94.4 (d, J = 1.8 Hz, C-10). ^{31}P NMR (161 MHz, $CDCl_3$): δ −69.54. HRMS (ESI$^+$): calcd for $C_{26}H_{18}O_2PS$ [M + H]$^+$, 425.0760; found, 425.0757. Mp: 195−196 °C. TLC: R_f = 0.36 (hexane/AcOEt = 10:1, UV). IR: ν (neat, cm^{-1}) 3066, 3051, 1590, 1487, 1457, 1282, 1243, 1227, 1187, 1149, 1070, 1018, 1001, 931, 909, 796, 768, 708, 686, 654, 637, 627, 611.

*9-Phospatriptycene (**1**).* For method A, to a solution of the 9-phospatriptycene-10-phenyl thiocarbonate **9** (2.43 g, 5.95 mmol, 1.0 equiv) in toluene (40 mL) were added AIBN (0.49 g, 2.98 mmol, 0.5 equiv) and TMS_3SiH (2.75 mL, 8.93 mmol, 1.5 equiv), and the reaction was stirred for 3 h at 80 °C. After the reaction cooled at room temperature, the solvent was evaporated and the resulting crude product was purified by flash chromatography (*n*-hexane/DCM = 20:1 to 10:1) giving a white solid (1.28 g, 4.7 mmol, 79%). Crystals suitable for X-ray diffraction analysis were obtained by slow evaporation of a saturated solution of 9-phosphatriptycene **1** in *n*-pentane. For method B, a solution of *t*BuLi in *n*-pentane (1.9 M, 1.36 mL, 2.6 mmol, 5.0 equiv) was added to a solution of tris(*ortho*-halogeno-phenyl)-methane **10** (0.3 g, 0.52 mmol, 1.0 equiv) at −110 °C in THF/Et_2O (1:1, 15 mL) over 15 min. Then the reaction mixture was stirred for 2 h at the same temperature. A solution of PCl_3 (45 μL in 1 mL of THF/Et_2O solution, 0.52 mmol, 1.0 equiv) was added dropwise (1 drop/min), and the reaction mixture was stirred for 2 h at −110 °C and was allowed to warm up to room temperature overnight. The solvents were removed under reduced pressure, and the resulting crude was purified by flash chromatography (*n*-hexane/DCM = 20:1 to 10:1) to give a white solid (88 mg, 0.32 mmol, 62%). The NMR data were in agreement with previously reported values.[6a] ^{1}H NMR (400 MHz, $CDCl_3$): δ 7.79 (t, J = 8.0 Hz, 3H, H-1, 8, 14), 7.53 (dd, J = 7.3 Hz, 3H, H-4, 5, 11), 7.18 (t, J = 7.4 Hz, 3H, H-3, 6, 12), 7.07 (t, J = 7.4 Hz, 3H, H-2, 7, 13), 5.60 (s, 1H, H-10). ^{13}C{^{1}H} NMR (100 MHz, $CDCl_3$): δ 149.4 (d, J = 3.5 Hz, C-4a, 5a, 10a), 141.0 (d, J = 8.8 Hz, C-8a, 9a, 14a), 132.6 (d, J = 36.4 Hz, C-1, 8, 14), 128.6 (d, J = 1.8 Hz, C-3, 6, 12), 125.8 (d, J = 1.4 Hz, C-4, 5, 11), 125.4 (d, J = 12.4 Hz, C-2, 7, 13), 59.9 (d, J = 1.2 Hz, C-10). ^{31}P NMR (161 MHz, CD_2Cl_2): δ − 64.35. HRMS (ESI$^+$): calcd for $C_{19}H_{14}P$ [M + H]$^+$, 273.0828; found, 273.0827. Mp: 227−228 °C (lit. 242−243 °C, from EtOH). TLC: R_f = 0.44 (cyclohexane/DCM = 15:1, UV). IR: ν (neat, cm^{-1}) 3061, 2995, 2949, 1597, 1491, 1445, 1245, 1128, 985, 862, 834, 741, 609.

*9-Phospatriptycene-tritylium Tetrafluoroborate Complex (**16**).* An NMR tube was charged with tritylium tetrafluoroborate (13.3 mg, 4.0 × 10^{-2} mmol), 9-phospatriptycene **1** (10 mg, 3.67 × 10^{-2} mmol), and 0.6 mL of CD_2Cl_2 in an argon glovebox. After measurements of the NMR spectra, the solvent was slowly evaporated under argon and the Lewis adduct **16** was obtained in a quantitative yield as pale yellow crystals suitable for single-crystal X-ray diffraction analysis. ^{1}H NMR (400 MHz, CD_2Cl_2): δ 7.92 (dd, J = 7.3, 4.6 Hz, 3H, H-4, 5, 11), 7.59 (dd, J = 8.3, 7.2 Hz, 3H, H-3, 6, 12), 7.54−7.22 (m, 15H, −C($C_6\underline{H}_5$)$_3$), 7.12−6.98 (m, 3H, H-2, 7, 13), 6.62−6.52 (m, 3H, H-1, 8, 14), 6.22 (s, 1H, H-10). ^{13}C{^{1}H} NMR (100 MHz, CD_2Cl_2): δ 149.0 (d, J = 2.8 Hz), 138.4 (d, J = 3.1 Hz), 132.9 (d, J = 2.5 Hz), 132.1 (d, J = 5.7 Hz), 131.0 (d, J = 6.8 Hz), 131.0, 130.7 (d, J = 1.1 Hz), 128.3 (d, J = 7.8 Hz), 127.5 (d, J = 11.4 Hz), 126.2, 125.5, 115.8, 64.2 (d, J = 41.6 Hz), 56.7 (d, J = 16.6 Hz). ^{31}P NMR (161 MHz, CD_2Cl_2): δ 4.18 ppm. HRMS (ESI$^+$): calcd for $C_{38}H_{28}P^+$ [M + H]$^+$, 515.1923; found, 515.1925.

*9-Phospatriptycene-tris(pentafluorophenyl)borane Complex (**18**).* An NMR tube was charged with tris(pentafluorophenyl)borane **17** (18.8 mg, 3.67 × 10^{-2} mmol), 9-phospatriptycene **1** (10 mg, 3.67 × 10^{-2} mmol), and 1 mL of CD_2Cl_2 in an argon atmosphere glovebox. The Lewis adduct **18** precipitated and crystallized rapidly in the NMR tube, and only the ^{1}H, ^{19}F, and ^{31}P could be recorded, whereas the ^{11}B and ^{13}C NMR spectra were not resolved because of the low concentration of **18** remaining in solution. The stability of **18** in CD_3CN or $CHCl_3$ was not sufficient for recording clean ^{11}B and ^{13}C NMR spectra. Crystals of **18** suitable for single-crystal X-ray diffraction analysis were obtained by slowly evaporating the CD_2Cl_2 solution in the glovebox. ^{1}H NMR (400 MHz, CD_2Cl_2): δ 7.65 (ddd, J = 7.6, 2.6, 1.3 Hz, 3H, H-1, 8, 14), 7.31 (t, J = 7.5 Hz, 3H, H-4, 5, 11), 7.00 (tdd, J = 7.6, 3.9, 1.3 Hz, 3H, H-3, 6, 12), 6.85 (t, J = 7.9 Hz, 3H, H-2, 7, 13), 5.68 (s, 1H, H-10). ^{31}P NMR (161 MHz, CD_2Cl_2): δ −35.8 ppm. ^{19}F NMR (378 MHz, CD_2Cl_2): −133.5 (m, 2F, meta), −154.2 (m, 1F, para), −163.7 (m, 2F, ortho).

■ ASSOCIATED CONTENT

Supporting Information

The Supporting Information is available free of charge on the ACS Publications website at DOI: 10.1021/acs.joc.9b01570.

Computational details, spectral data, and X-ray crystallographic information for compounds (PDF)
Crystal data for compound **1** (CIF)
Crystal data for compound **1**, 100 K (CIF)
Crystal data for compound **8** (CIF)
Crystal data for compound **9** (CIF)
Crystal data for compound **16** (CIF)
Crystal data for compound **18** (CIF)

Accession Codes

CCDC 1905038−40, 1905042, 1905043, and 1906080 contain the supplementary crystallographic data. These data can be obtained free of charge via www.ccdc.cam.ac.uk/data_request/cif, or by e-mailing data_request@ccdc.cam.ac.uk.

■ AUTHOR INFORMATION

Corresponding Authors

*E-mail: raphael.robiette@uclouvain.be.
*E-mail: guillaume.berionni@unamur.be.

ORCID

Nikolay Tumanov: 0000-0001-6898-9036
Raphaël Robiette: 0000-0002-3449-565X
Guillaume Berionni: 0000-0002-5422-9113

Notes

The authors declare no competing financial interest.

■ ACKNOWLEDGMENTS

We acknowledge the University of Namur, the Namur Institute of Structured Matter (NISM), and the Fond National de la Recherche Scientifique FNRS (MIS grant F.4513.18 for G.B.)

DOI: 10.1021/acs.joc.9b01570
J. Org. Chem. 2019, 84, 11268−11274

for generous funding. We thank the PC^2 technological platform at the University of Namur for access to X-ray diffraction and NMR instruments. We thank Dr. Koen Robeyns (UCLouvain) for the help with refinement of **18**. Computational resources have been provided by the supercomputing facilities of the Université catholique de Louvain (CISM/UCL) and the Consortium des Équipements de Calcul Intensif en Fédération Wallonie Bruxelles (CÉCI) funded by the FNRS under convention 2.5020.11 and by the Walloon Region. L.H. was supported through a Ph.D. grant from the China Scholarship Council (CSC, 201606670003). R.R. is a Maître de Recherche of the F.R.S.-FNRS.

REFERENCES

(1) (a) Iaroshenko, V., Ed; *Organophosphorus Chemistry: From Molecules to Applications*; Wiley-VCH, 2019. (b) Kamer, P. C.; Van Leeuwen, P. W., Ed; *Phosphorus(III) Ligands in Homogeneous Catalysis: Design and Synthesis*; Wiley: Chichester, 2012.

(2) (a) Guo, H.; Fan, Y. C.; Sun, Z.; Wu, Y.; Kwon, O. Phosphine Organocatalysis. *Chem. Rev.* **2018**, *118* (20), 10049−10293. (b) Methot, J. L.; Roush, W. R. Nucleophilic Phosphine Organocatalysis. *Adv. Synth. Catal.* **2004**, *346*, 1035−1050.

(3) Lam, J.; Szkop, K. M.; Mosaferi, E.; Stephan, D. W. FLP Catalysis: Main Group Hydrogenations of Organic Unsaturated Substrates. *Chem. Soc. Rev.* **2019**, *48*, 3592−3612.

(4) For a recent review on phosphines reactivity, see: Durand, D. J.; Fey, N. Computational Ligand Descriptors for Catalyst Design. *Chem. Rev.* **2019**, *119*, 6561−6594.

(5) For phospha-angulenes, see: (a) Yamamura, M.; Hasegawa, T.; Nabeshima, T. Synthesis of Phosphorus-Centered and Chalcogen-Bridged Concave Molecules: Modulation of Bowl Geometries and Packing Structures by Changing Bridging Atoms. *Org. Lett.* **2016**, *18*, 816−819. (b) Hirai, S.; Tanaka, N.; Sakai, M.; Yamaguchi, S. Structurally Constrained Boron-, Nitrogen-, Silicon-, and Phosphorus-Centered Polycyclic π-Conjugated Systems. *Chem. Rev.* **2019**, *119*, 8291−8331. For phospha-norbornadienes, see: (c) Robin, F.; Lelièvre, S.; Mercier, F.; Ricard, L.; Mathey, F. 1-Phosphanorbornadienes in Enantioselective Catalysis. *Phosphorus, Sulfur Silicon Relat. Elem.* **2002**, *177*, 1371−1374. For phospha-barrelenes, see: (d) Fuchs, E.; Keller, M.; Breit, B. Phosphabarrelenes as Ligands in Rhodium-Catalyzed Hydroformylation of Internal Alkenes Essentially Free of Alkene Isomerization. *Chem. - Eur. J.* **2006**, *12*, 6930−6939. For phospha-adamantanes, see: (e) Brenstrum, T.; Gerristma, D. A.; Adjabeng, G. M.; Frampton, C. S.; Britten, J.; Robertson, A. J.; McNulty, J.; Capretta, A. Phosphaadamantanes as Ligands for Palladium Catalyzed Cross-Coupling Chemistry: Library Synthesis, Characterization, and Screening in the Suzuki Coupling of Alkyl Halides and Tosylates Containing β-Hydrogens with Boronic Acids and Alkylboranes. *J. Org. Chem.* **2004**, *69*, 7635−7639.

(6) (a) Jongsma, C.; de Kleijn, J. P.; Bickelhaupt, F. Phosphatriptycene. *Tetrahedron* **1974**, *30*, 3465−3469. (b) Kobayashi, J.; Agou, T.; Kawashima, T. A Novel and Convenient Synthetic Route to a 9-Phosphatriptycene and Systematic Comparisons of 9-Phosphatriptycene Derivatives. *Chem. Lett.* **2003**, *32* (12), 1144−1145. (c) Agou, T.; Kobayashi, J.; Kawashim, T. Synthesis, Structure, and Reactivity of a Symmetrically Substituted 9-Phosphatriptycene Oxide and Its Derivatives. *Heteroat. Chem.* **2004**, *15* (6), 437−446.

(7) (a) Tsuji, H.; Inoue, T.; Kaneta, Y.; Sase, S.; Kawachi, A.; Tamao, K. Synthesis, Structure, and Properties of 9-Phospha-10-silatriptycenes and their Derivatives. *Organometallics* **2006**, *25*, 6142−6148. (b) Agou, T.; Kobayashi, J.; Kawashima, T. Evaluation of t-Donating Ability of a 9-Phosphatriptycene and Its Application to Catalytic Reactions. *Chem. Lett.* **2004**, *33*, 1028−1029.

(8) (a) Konishi, S.; Iwai, T.; Sawamura, M. Synthesis, Properties, and Catalytic Application of a Triptycene-Type Borate-Phosphine Ligand. *Organometallics* **2018**, *37*, 1876−1883. (b) Iwai, T.; Konishi, S.; Miyazaki, T.; Kawamorita, S.; Yokokawa, N.; Ohmiya, H.; Sawamura, M. Silica-Supported Triptycene-Type Phosphine. Synthesis, Characterization, and Application to Pd-Catalyzed Suzuki-Miyaura Cross-Coupling of Chloroarenes. *ACS Catal.* **2015**, *5*, 7254−7264.

(9) (a) Cao, Y.; Napoline, J. W.; Bacsa, J.; Pollet, P.; Soper, J. D.; Sadighi, J. P. Synthesis of an Azaphosphatriptycene and Its Rhodium Carbonyl Complex. *Organometallics* **2019**, *38*, 1868−1871. For the synthesis of the parent 9-aza-10-phosphatriptycene, see: (b) Hellwinkel, D.; Schenk, W. Azaphosphatriptycene. *Angew. Chem., Int. Ed. Engl.* **1969**, *8*, 987−988.

(10) Ube, H.; Yasuda, Y.; Sato, H.; Shionoya, M. Metal-Centred AzaphosphatriptyceneGear with a Photo- and Thermally Driven Mechanical Switching Function Based on Coordination Isomerism. *Nat. Commun.* **2017**, *8*, 14296.

(11) Drover, M. W.; Nagata, K.; Peters, J. C. Fusing Triphenylphosphine with Tetraphenylborate: Introducing the 9-Phosphatriptycene-10-phenylborate (PTB) Anion. *Chem. Commun.* **2018**, *54*, 7916−7919.

(12) Sadighi, J. P. New Ligands for Catalysis Through Elaboration of the Phosphatriptycene Framework. *PRF Annual Report* **2016**, 54739−ND3.

(13) Hellwinkel, D.; Schenk, W.; Blaicher, W. Heterotriptycene; Strukturberechnungen und Kernresonanzrelationen. *Chem. Ber.* **1978**, *111*, 1798−1814.

(14) Creutz, S. E.; Peters, J. C. Catalytic Reduction of N_2 to NH_3 by an Fe-N_2 Complex Featuring a C-Atom Anchor. *J. Am. Chem. Soc.* **2014**, *136*, 1105−1115.

(15) (a) Tolman, C. A. Steric Effects of Phosphorus Ligands in Organometallic Chemistry and Homogeneous Catalysis. *Chem. Rev.* **1977**, *77*, 313−348. (b) Müller, T. E.; Mingos, D. M. P. Determination of the Tolman Cone Angle from Crystallographic Parameters and a Statistical Analysis Using the Crystallographic Database. *Transition Met. Chem.* **1995**, *20*, 533−539.

(16) Jover, J.; Fey, N.; Purdie, M.; Lloyd-Jones, G. C.; Harvey, J. N. A Computational Study of Phosphine Ligand Effects in Suzuki-Miyaura Coupling. *J. Mol. Catal. A: Chem.* **2010**, *324*, 39−47.

(17) For a recent study with a similar observation for azaphosphatriptycene, see ref 9a.

(18) Serron, S.; Huang, J.; Nolan, S. P. Solution Thermochemical Study of Tertiary Phosphine Ligand Substitution Reactions in the Rh(acac)(CO)(PR_3) System. *Organometallics* **1998**, *17*, 534−539.

(19) Calculations were carried out at the M06-2X/6-311+G**(benzene)//B3LYP-D3/6-31+G* level of theory using the Jaguar 8.5 pseudospectral program package. See the Supporting Information for full computational details.

(20) Poë, A. J.; Farrar, D. H.; Zheng, Y. Systematic Kinetics of High Nuclearity Metal Carbonyl Clusters. Associative Substitution Reactions of $Ru_6C(CO)_{17}$ with P-donor Nucleophiles. *J. Am. Chem. Soc.* **1992**, *114*, 5146−5152.

(21) (a) Mayr, H.; Ofial, A. R. Philicities, Fugalities, and Equilibrium Constants. *Acc. Chem. Res.* **2016**, *49*, 952−965. (b) Mayr, H.; Ammer, J.; Baidya, M.; Maji, B.; Nigst, T. A.; Ofial, A. R.; Singer, T. Scales of Lewis basicities toward C-centered Lewis acids (carbocations). *J. Am. Chem. Soc.* **2015**, *137*, 2580−2599. (c) Follet, E.; Mayer, P.; Stephenson, D. S.; Ofial, A. R.; Berionni, G. Reactivity-Tuning in Frustrated Lewis Pairs: Nucleophilicity and Lewis Basicity of Sterically Hindered Phosphines. *Chem. - Eur. J.* **2017**, *23*, 7422−7427.

(22) *Jaguar*, version 8.5; Schrodinger, Inc.: New York, 2014.

(23) (a) Becke, A. D. Density-functional thermochemistry. III. The role of exact exchange. *J. Chem. Phys.* **1993**, *98*, 5648−5652. (b) Stephens, P. J.; Devlin, F. J.; Chabalowski, C. F.; Frisch, M. J. Ab Initio Calculation of Vibrational Absorption and Circular Dichroism Spectra Using Density Functional Force Fields. *J. Phys. Chem.* **1994**, *98*, 11623−11627.

(24) (a) Grimme, S.; Antony, J.; Ehrlich, S.; Krieg, H. A Consistent and Accurate Ab Initio Parametrization of Density Functional Dispersion Correction (DFT-D) for the 94 Elements H-Pu. *J. Chem. Phys.* **2010**, *132*, 154104. (b) Goerigk, L.; Grimme, S. A Thorough Benchmark of Density Functional Methods for General

DOI: 10.1021/acs.joc.9b01570
J. Org. Chem. 2019, 84, 11268−11274

Main Group Thermochemistry, Kinetics, and Noncovalent Interactions. *Phys. Chem. Chem. Phys.* **2011**, *13*, 6670−6688.
(25) Hehre, W. J.; Ditchfield, R.; Pople, J. A. *J. Chem. Phys.* **1972**, *56*, 2257−2261.
(26) Fey, N.; Tsipis, A. C.; Harris, S. E.; Harvey, J. N.; Orpen, A. G.; Mansson, R. A. Development of a Ligand Knowledge Base, Part 1: Computational Descriptors for Phosphorus Donor Ligands. *Chem. - Eur. J.* **2006**, *12*, 291−302.
(27) *CrysAlis PRO*; Rigaku Oxford Diffraction: Oxford, 2018.
(28) Sheldrick, G. M. SHELXT - Integrated space-group and crystal-structure determination. *Acta Crystallogr., Sect. A: Found. Adv.* **2015**, *71*, 3−8.
(29) Sheldrick, G. M. Crystal Structure Refinement With SHELXL. *Acta Crystallogr., Sect. C: Struct. Chem.* **2015**, *71*, 3−8.
(30) Dolomanov, O. V.; Bourhis, L. J.; Gildea, R. J.; Howard, J. A. K.; Puschmann, H. *OLEX2*: AComplete Structure Solution, Refinement and Analysis Program. *J. Appl. Crystallogr.* **2009**, *42*, 339−341.
(31) Hübschle, C. B.; Sheldrick, G. M.; Dittrich, B. ShelXle: A Qt Graphical User Interface for SHELXL. *J. Appl. Crystallogr.* **2011**, *44*, 1281−1284.
(32) Macrae, C. F.; Bruno, I. J.; Chisholm, J. A.; Edgington, P. R.; McCabe, P.; Pidcock, E.; Rodriguez-Monge, L.; Taylor, R.; van de Streek, J.; Wood, P. A. Mercury CSD 2.0 - New Features for the Visualisation and Investigation of Crystal Structures. *J. Appl. Crystallogr.* **2008**, *41*, 466−470.

DOI: 10.1021/acs.joc.9b01570
J. Org. Chem. 2019, 84, 11268−11274